

Two-species fermion mixtures with population imbalance

M. Iskin and C. A. R. Sá de Melo

School of Physics, Georgia Institute of Technology, Atlanta, Georgia 30332, USA

(Dated: March 5, 2018)

We analyze the phase diagram of uniform superfluidity for two-species fermion mixtures from the Bardeen-Cooper-Schrieffer (BCS) to Bose-Einstein condensation (BEC) limit as a function of the scattering parameter and population imbalance. We find at zero temperature that the phase diagram of population imbalance versus scattering parameter is asymmetric for unequal masses, having a larger stability region for uniform superfluidity when the lighter fermions are in excess. In addition, we find topological quantum phase transitions associated with the disappearance or appearance of momentum space regions of zero quasiparticle energies. Lastly, near the critical temperature, we derive the Ginzburg-Landau equation, and show that it describes a dilute mixture of composite bosons and unpaired fermions in the BEC limit.

PACS numbers: 03.75.Ss, 03.75.Hh, 05.30.Fk

Major experimental breakthroughs have been made recently involving one-species trapped fermions (${}^6\text{Li}$) in two hyperfine states with different populations. The superfluid to normal phase transition and the vortex state [1], as well as phase separation between paired and unpaired fermions [2] were identified as a function of population imbalance and scattering parameter. These studies are important extensions of the so-called Bardeen-Cooper-Schrieffer (BCS) to Bose-Einstein condensation (BEC) evolution for equal populations, which were studied via the use of Feshbach resonances [3, 4, 5, 6, 7, 8]. The problem of fermion superfluidity with population imbalance has been revisited recently in several theoretical works in continuum [9, 10, 11, 12, 13, 14, 15, 16, 17, 18, 19] and trapped [20, 21, 22, 23, 24, 25, 26] atoms. These one-species experiments are ideal candidates for the observation of uniform and non-uniform superfluid phases, which may be present not only in atomic, but also in nuclear (pairing in nuclei), astrophysics (neutron stars), and condensed matter (superconductors) systems.

Arguably one of the next frontiers of exploration in ultracold Fermi systems is the search for superfluidity in two-species fermion mixtures (e.g. ${}^6\text{Li}$ and ${}^{40}\text{K}$) with and without population imbalance. While earlier works on two-species fermion mixtures were limited to the BCS limit [9, 10], in this manuscript we study the evolution of superfluidity from the BCS to the BEC limit as a function of the scattering parameter and population imbalance.

Our main results are as follows. At zero temperature, we construct the phase diagram for equal and unequal masses of paired fermions as a function of scattering parameter and population imbalance $P = (N_\uparrow - N_\downarrow)/(N_\uparrow + N_\downarrow)$ as shown in Fig. 1. The phase diagram is asymmetric for unequal masses, having a larger stability region for uniform superfluidity when the population N_\uparrow of lighter fermions is larger than the population N_\downarrow of heavier fermions. In addition, we find topological quantum phase transitions in the phase diagram associated with the disappearance or appearance of momentum space re-

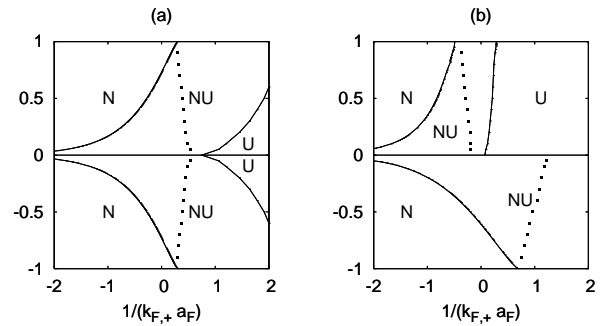


FIG. 1: Phase diagram of $P = (N_\uparrow - N_\downarrow)/(N_\uparrow + N_\downarrow)$ versus $1/(k_{F,+} a_F)$ for a) equal ($m_\uparrow = m_\downarrow$) and b) unequal masses ($m_\uparrow = 0.15m_\downarrow$). We show normal (N), non-uniform (NU) or uniform (U) superfluid phases. The dotted and $P = 0$ lines separate topologically distinct regions. In b) the U phase also occurs for $P < 0$ when $1/(k_{F,+} a_F) > 4.8$ (not shown).

gions of zero quasiparticle energies. Lastly, near the critical temperature, we derive the time-dependent Ginzburg-Landau (TDGL) equation, and show that it describes a dilute mixture of bosons (tightly bound fermions) and excess (unpaired) fermions in the BEC limit.

To describe a dilute two-species Fermi gas in three dimensions, we start from the Hamiltonian ($\hbar = 1$)

$$H = \sum_{\mathbf{k},\sigma} \xi_{\mathbf{k},\sigma} a_{\mathbf{k},\sigma}^\dagger a_{\mathbf{k},\sigma} + \sum_{\mathbf{k},\mathbf{k}',\mathbf{q}} V(\mathbf{k},\mathbf{k}') b_{\mathbf{k},\mathbf{q}}^\dagger b_{\mathbf{k}',\mathbf{q}}, \quad (1)$$

where the pseudo-spin σ labels the hyperfine states represented by the creation operator $a_{\mathbf{k},\sigma}^\dagger$, and $b_{\mathbf{k},\mathbf{q}}^\dagger = a_{\mathbf{k}+\mathbf{q}/2,\uparrow}^\dagger a_{-\mathbf{k}+\mathbf{q}/2,\downarrow}^\dagger$. Here, $\xi_{\mathbf{k},\sigma} = \epsilon_{\mathbf{k},\sigma} - \mu_\sigma$, where $\epsilon_{\mathbf{k},\sigma} = k^2/(2m_\sigma)$ is the energy and μ_σ is the chemical potential of the fermions. Notice that, we allow for the fermions to have different masses m_σ and different populations controlled by independent chemical potentials μ_σ . The attractive fermion-fermion interaction $V(\mathbf{k},\mathbf{k}')$ can be written in a separable form as $V(\mathbf{k},\mathbf{k}') = -g\Gamma_{\mathbf{k}}^* \Gamma_{\mathbf{k}'}$ where $g > 0$, and $\Gamma_{\mathbf{k}} = 1$ for the s-wave symmetry.

The gaussian effective action for H is [27] $S_{\text{gauss}} = S_0 + (\beta/2) \sum_q \bar{\Lambda}^\dagger(q) \mathbf{F}^{-1}(q) \bar{\Lambda}(q)$, where $q = (\mathbf{q}, v_\ell)$ with bosonic Matsubara frequency $v_\ell = 2\ell\pi/\beta$. Here, $\beta = 1/T$, $\bar{\Lambda}^\dagger(q)$ is the order parameter fluctuation field, and the matrix $\mathbf{F}^{-1}(q)$ is the inverse fluctuation propagator. The saddle point action is

$$S_0 = \beta \frac{|\Delta_0|^2}{g} + \sum_{\mathbf{k}} \{ \beta(\xi_{\mathbf{k},+} - E_{\mathbf{k},+}) + \ln[n_F(-E_{\mathbf{k},\uparrow})] + \ln[n_F(-E_{\mathbf{k},\downarrow})] \}, \quad (2)$$

where $E_{\mathbf{k},\sigma} = (\xi_{\mathbf{k},+}^2 + |\Delta_{\mathbf{k}}|^2)^{1/2} + s_\sigma \xi_{\mathbf{k},-}$ is the quasiparticle energy when $s_\uparrow = 1$ and the negative of the quasi-hole energy when $s_\downarrow = -1$, and $E_{\mathbf{k},\pm} = (E_{\mathbf{k},\uparrow} \pm E_{\mathbf{k},\downarrow})/2$. Here, $\Delta_{\mathbf{k}} = \Delta_0 \Gamma_{\mathbf{k}}$ is the order parameter, $n_F(E_{\mathbf{k},\sigma})$ is the Fermi distribution and $\xi_{\mathbf{k},\pm} = (\xi_{\mathbf{k},\uparrow} \pm \xi_{\mathbf{k},\downarrow})/2 = k^2/(2m_\pm) - \mu_\pm$, where $m_\pm = 2m_\uparrow m_\downarrow / (m_\downarrow \pm m_\uparrow)$ and $\mu_\pm = (\mu_\uparrow \pm \mu_\downarrow)/2$. Notice that m_+ is twice the reduced mass of the \uparrow and \downarrow fermions, and that the equal mass case corresponds to $|m_-| \rightarrow \infty$. The fluctuation term in the action leads to a correction to the thermodynamic potential, which can be written as $\Omega_{\text{gauss}} = \Omega_0 + \Omega_{\text{fluct}}$ with $\Omega_0 = S_0/\beta$ and $\Omega_{\text{fluct}} = (1/\beta) \sum_q \ln \det[\mathbf{F}^{-1}(q)/\beta]$.

The saddle point condition $\delta S_0 / \delta \Delta_0^* = 0$ leads to an equation for the order parameter

$$\frac{1}{g} = \sum_{\mathbf{k}} \frac{|\Gamma_{\mathbf{k}}|^2}{2E_{\mathbf{k},+}} \mathcal{X}_{\mathbf{k},+}, \quad (3)$$

where $\mathcal{X}_{\mathbf{k},\pm} = (\mathcal{X}_{\mathbf{k},\uparrow} \pm \mathcal{X}_{\mathbf{k},\downarrow})/2$ with $\mathcal{X}_{\mathbf{k},\sigma} = \tanh(\beta E_{\mathbf{k},\sigma}/2)$. As usual, we eliminate g in favor of the scattering length a_F via the relation $1/g = -m_+ V / (4\pi a_F) + \sum_{\mathbf{k}} |\Gamma_{\mathbf{k}}|^2 / (2\epsilon_{\mathbf{k},+})$, where $\epsilon_{\mathbf{k},\pm} = (\epsilon_{\mathbf{k},\uparrow} \pm \epsilon_{\mathbf{k},\downarrow})/2$. The order parameter equation has to be solved self-consistently with number equations $N_\sigma = -\partial\Omega/\partial\mu_\sigma$ which have two contributions $N_\sigma = N_{0,\sigma} + N_{\text{fluct},\sigma}$. $N_{0,\sigma}$ is the saddle point number equation given by

$$N_{0,\sigma} = -\frac{\partial\Omega_0}{\partial\mu_\sigma} = \sum_{\mathbf{k}} \left(\frac{1 - s_\sigma \mathcal{X}_{\mathbf{k},-}}{2} - \frac{\xi_{\mathbf{k},+}}{2E_{\mathbf{k},+}} \mathcal{X}_{\mathbf{k},+} \right) \quad (4)$$

and $N_{\text{fluct},\sigma} = -\partial\Omega_{\text{fluct}}/\partial\mu_\sigma$ is the fluctuation contribution to N given by $N_{\text{fluct},\sigma} = -(1/\beta) \sum_q \{ \partial[\det \mathbf{F}^{-1}(q)] / \partial\mu_\sigma \} / \det \mathbf{F}^{-1}(q)$. We define $B_\pm = m_\uparrow \mu_\uparrow \pm m_\downarrow \mu_\downarrow$ to establish general constraints on the magnitude $|\Delta_0|$ of the order parameter for s-wave pairing in the presence of population imbalance ($N_\uparrow \neq N_\downarrow$). Population imbalance is achieved when either $E_{\mathbf{k},\uparrow}$ or $E_{\mathbf{k},\downarrow}$ is negative in some regions of momentum space. Depending on the number of zeros of $E_{\mathbf{k},\uparrow}$ and $E_{\mathbf{k},\downarrow}$ (zero energy surfaces in momentum space), there are two topologically distinct cases: (I) $E_{\mathbf{k},\sigma}$ has no zeros and $E_{\mathbf{k},-\sigma}$ has only one, and (II) $E_{\mathbf{k},\sigma}$ has no zeros and $E_{\mathbf{k},-\sigma}$ has two zeros. The zeros of $E_{\mathbf{k},\sigma}$ occur at real momenta $k_\pm^2 = B_\pm \pm (B_\pm^2 - 4m_\uparrow m_\downarrow |\Delta_0|^2)^{1/2}$ provided that $|\Delta_0|^2 < |B_-|^2 / (4m_\uparrow m_\downarrow)$ for $B_+ \geq 0$

and $|\Delta_0|^2 < -\mu_\uparrow \mu_\downarrow$ for $B_+ < 0$. The $P = 0$ limit corresponds to case (III), where $E_{\mathbf{k},\sigma}$ has no zeros and is always positive. We illustrate these cases in Fig. 2 for $N_\uparrow > N_\downarrow$. Notice that, the Fermi sea of the lower quasiparticle band is a sphere of radius k_+ in case (I), and is a spherical shell $k_- \leq k \leq k_+$ in case (II). The transition from case (II) to case (I) occurs when $k_- \rightarrow 0$, indicating a change in topology in the lowest quasiparticle band, similar to the Lifshitz transition in ordinary metals and non-s-wave superfluids [28, 29]. The topological transition here is unique, because it involves an s-wave superfluid, and could be potentially observed for the first time through the measurement of the momentum distribution.

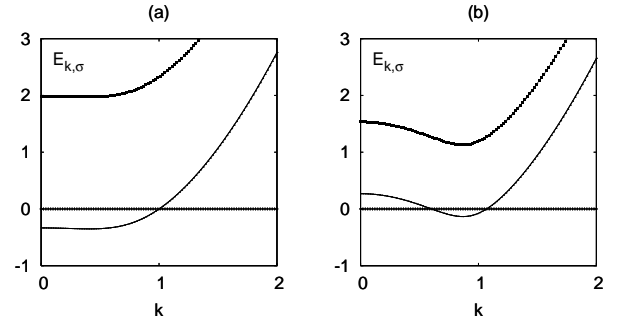


FIG. 2: Schematic plots of $E_{\mathbf{k},\uparrow}$ (dotted lines) and $E_{\mathbf{k},\downarrow}$ (solid lines) versus k a) for case (I), and b) for case (II).

The $T = 0$ momentum distributions for cases (I) and (II) can be obtained from Eq. 4. For momentum space regions where $E_{\mathbf{k},\sigma} > 0$ and $E_{\mathbf{k},-\sigma} > 0$, the corresponding momentum distributions are equal $n_{\mathbf{k},\sigma} = n_{\mathbf{k},-\sigma}$. However, when $E_{\mathbf{k},\sigma} > 0$ and $E_{\mathbf{k},-\sigma} < 0$, then $n_{\mathbf{k},\sigma} = 0$ and $n_{\mathbf{k},-\sigma} = 1$. Although this topological transition is quantum ($T = 0$) in nature, signatures of the transition should still be observed at finite temperatures within the quantum critical region, where the momentum distributions are smeared out due to thermal effects. Although the primary signature of this topological transition is seen in the momentum distribution, the isentropic κ_S or isothermal κ_T compressibilities and the speed of sound c_s would have a cusp at the topological transition line similar to that encountered in $|\Delta_0|$ (see Fig. 3) as a function of the scattering parameter $1/(k_{F,+} a_F)$. The cusp (discontinuous change in slope) in κ_S , κ_T or c_s gets larger with increasing population imbalance.

Next, we solve Eqs (3) and (4) to analyze the phase diagram at $T = 0$ as a function of scattering parameter $1/(k_{F,+} a_F)$ and population imbalance $P = N_-/N_+$, where $N_\pm = (N_\uparrow \pm N_\downarrow)/2$ and $k_{F,\pm}^3 = (k_{F,\uparrow}^3 \pm k_{F,\downarrow}^3)/2$. We perform calculations for equal ($m_\uparrow = m_\downarrow$) and unequal ($m_\uparrow = 0.15m_\downarrow$) masses cases, corresponding to one-species (${}^6\text{Li}$ or ${}^{40}\text{K}$ only), and two-species (${}^6\text{Li}$ and ${}^{40}\text{K}$ mixture) experiments, respectively.

For $T \approx 0$, $N_{\text{fluct},\sigma}$ is small compared to $N_{0,\sigma}$ for

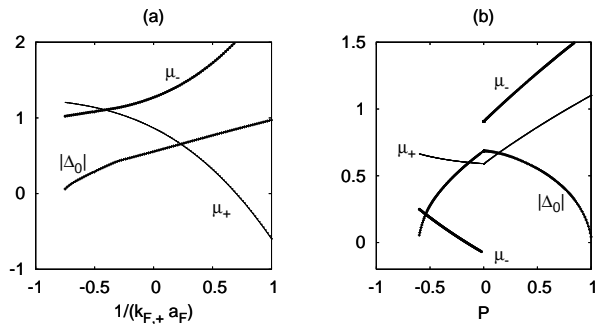


FIG. 3: Plots of $|\Delta_0|$, μ_+ and μ_- (units of $\epsilon_{F,+}$) for $m_\uparrow = 0.15m_\downarrow$ a) as a function of $1/(k_{F,+}a_F)$ when $P = 0.5$ and b) as a function of P when $1/(k_{F,+}a_F) = 0$.

all $1/(k_{F,+}a_F)$ leading to $N_\sigma \approx N_{0,\sigma}$ [30]. We define $\epsilon_{F,\pm} = k_{F,\pm}^2/(2m_\pm)$ and in Fig. 3, we plot self-consistent solutions of $|\Delta_0|$, μ_+ and μ_- (in units of $\epsilon_{F,+}$) at $T = 0$ for two cases: a) as a function of $1/(k_{F,+}a_F)$ when $P = 0.5$ (or $N_\uparrow = 3N_\downarrow$) and b) as a function of P when $1/(k_{F,+}a_F) = 0$ (or on resonance).

In Fig. 3a, the BCS $\mu_\pm \approx (\epsilon_{F,\uparrow} \pm \epsilon_{F,\downarrow})/2$ changes continuously to the BEC $|\mu_\pm| \rightarrow |\epsilon_b|/2$, where $\epsilon_b = -1/(m_+a_F^2)$ is the binding energy which follows from $1/g = \sum_{\mathbf{k}} |\Gamma_{\mathbf{k}}|^2 / (2\epsilon_{\mathbf{k},+} - \epsilon_b)$. Since $P > 0$ and the \uparrow fermions are in excess, all \downarrow fermions pair to form N_\downarrow bosons and the remaining \uparrow fermions are unpaired. The amplitude $|\Delta_0|$ evolves continuously from the BCS to the BEC limit with a cusp around $1/(k_{F,+}a_F) \approx -0.27$. This cusp in $|\Delta_0|$ is more pronounced for higher $|P|$ and signals a quantum phase transition from case (I) to case (II), which can be detected experimentally [8].

In Fig. 3b, we show (on resonance) that $|\Delta_0| = 0$ (normal phase) for $P < -0.61$, where $\mu_+ \approx 0.64\epsilon_{F,+}$ and $\mu_- \approx 0.28\epsilon_{F,+}$. We notice that the evolution of $|\Delta_0|$, μ_+ and μ_- as a function of P is non-analytic when $|P| \rightarrow 0$, and signals a quantum phase transition from case (II) with $P > 0$ to case (III) with $P = 0$ to case (I) with $P < 0$. We obtain similar results when $m_\uparrow = m_\downarrow$, where the plot is symmetric around $P = 0$. Therefore, this quantum phase transition may be studied in current experiments involving only one-species of fermions [1, 2].

Next, we discuss the stability of uniform superfluidity using two criteria. The first criterion requires that the curvature $\partial^2\Omega_0/\partial\Delta_0^2$ of the saddle point free energy $\Omega_0 = S_0/\beta$ with respect to Δ_0 to be positive. When $\partial^2\Omega_0/\partial\Delta_0^2$ is negative, the uniform saddle point solution does not correspond to a minimum of Ω_0 , and a non-uniform superfluid phase is favored. The second criterion requires the eigenvalues of the superfluid density

$$\rho_{ij}(T) = (m_\uparrow N_\uparrow + m_\downarrow N_\downarrow)\delta_{ij} - \frac{\beta}{2} \sum_{\mathbf{k}} k_i k_j \mathcal{Y}_{\mathbf{k},+} \quad (5)$$

to be positive. Here, δ_{ij} is the Kronecker delta, and $\mathcal{Y}_{\mathbf{k},\pm} = (\mathcal{Y}_{\mathbf{k},\uparrow} \pm \mathcal{Y}_{\mathbf{k},\downarrow})/2$, with $\mathcal{Y}_{\mathbf{k},\sigma} = \text{sech}^2(\beta E_{\mathbf{k},\sigma}/2)$.

When at least one of the eigenvalues of $\rho_{ij}(T)$ is negative, a spontaneously generated gradient of the phase of the order parameter appears, leading to a non-uniform superfluid phase. Notice that, $\rho_{ij}(T)$ reduces to a scalar $\rho_0(T)$ for s-wave systems.

The uniform superfluid (U) phase is characterized by $\rho_0(0) > 0$ and $\partial^2\Omega_0/\partial\Delta_0^2 > 0$, and the normal (N) phase is characterized by $\Delta_0 = 0$. The non-uniform superfluid (NU) phase is characterized by $\rho_0(0) < 0$ and/or $\partial^2\Omega_0/\partial\Delta_0^2 < 0$. The NU phase should be of the LOFF-type having one wavevector modulation for the center of mass momentum of a Cooper pair near the BCS limit, where pairing occurs within a very narrow region around the lowest Fermi energy of either the lighter or heavier atom. Towards unitarity and beyond, we expect the NU phase to be substantially different from LOFF phases having spatial modulation that would encompass several wavevectors. This expectation is based on the idea that when the attraction between fermions gets stronger, the Fermi mixture becomes more non-degenerate, and there is a wider region in energy within which pairing can occur, leading to a range of possible wavevectors for the center of mass momentum of Cooper pairs.

As shown in Fig. 1a, when $m_\uparrow = m_\downarrow$, the phase diagram is symmetric around $P = 0$. A continuous quantum phase transition occurs from the NU to the N phase beyond a critical population imbalance on the BCS side. In addition, a discontinuous transition from the NU to the U phase of topological type (I) also occurs.

In contrast, as shown in Fig. 1b, when $m_\uparrow = 0.15m_\downarrow$, the phase diagram is asymmetric around $P = 0$. A continuous quantum phase transition occurs from the NU to the N phase beyond a critical population imbalance on the BCS side. Furthermore, it is found that the U phase has a larger stability region when light fermions are in excess, and that a discontinuous transition from the NU to the U phase occurs. The U phase also exists for $P < 0$ when $1/(k_{F,+}a_F) > 4.8$ (not shown). Lastly, one of the topological quantum phase transitions (dotted lines) is very close to the NU/U boundary for $P > 0$ in contrast to the equal mass case. This line indicates a change in quasiparticle Fermi surface topology from type (I) to type (II), and may lie in the U region when $m_\uparrow/m_\downarrow < 0.15$.

Next, we discuss superfluidity near $T \approx T_c$, where $\Delta_0 = 0$, and derive the TDGL equation [31]. We use the small \mathbf{q} and $i\nu_\ell \rightarrow \omega + i\delta$ expansion of

$$L^{-1}(q) = \frac{1}{g} - \sum_{\mathbf{k}} \frac{1 - n_F(\xi_{\mathbf{k}+\mathbf{q}/2,\uparrow}) - n_F(\xi_{\mathbf{k}-\mathbf{q}/2,\downarrow})}{\xi_{\mathbf{k}+\mathbf{q}/2,\uparrow} + \xi_{\mathbf{k}-\mathbf{q}/2,\downarrow} - i\nu_\ell} |\Gamma_{\mathbf{k}}|^2,$$

where $L^{-1}(q) = \mathbf{F}_{11}^{-1}(q)$, to obtain the TDGL equation

$$\left[a + b|\Lambda(x)|^2 - \sum_{i,j} \frac{c_{ij}}{2} \nabla_i \nabla_j - id \frac{\partial}{\partial t} \right] \Lambda(x) = 0 \quad (6)$$

in the real space $x = (\mathbf{x}, t)$ representation. The coefficients are given by $a = 1/g - \sum_{\mathbf{k}} X_{\mathbf{k},+} |\Gamma(\mathbf{k})|^2 / (2\xi_{\mathbf{k},+})$,

which leads to the saddle equation when $a = 0$ (Thouless condition), and $c_{ij} = \sum_{\mathbf{k}} \{ \beta^2 k_i k_j (X_{\mathbf{k},\uparrow} Y_{\mathbf{k},\uparrow} / m_{\uparrow}^2 + X_{\mathbf{k},\downarrow} Y_{\mathbf{k},\downarrow} / m_{\downarrow}^2) / (32\xi_{\mathbf{k},+}) + \beta(k_i k_j C_- / (m_- \xi_{\mathbf{k},+}) - \delta_{ij} C_+ / 2) (8\xi_{\mathbf{k},+}) + X_{\mathbf{k},+} [\delta_{ij} / (2m_+) - k_i k_j / (m_-^2 \xi_{\mathbf{k},+})] / (4\xi_{\mathbf{k},+}^2) \} |\Gamma_{\mathbf{k}}|^2$, where $C_{\pm} = (Y_{\mathbf{k},\uparrow} / m_{\uparrow} \pm Y_{\mathbf{k},\downarrow} / m_{\downarrow}) / 2$, $X_{\mathbf{k},\sigma} = \tanh(\beta\xi_{\mathbf{k},\sigma} / 2)$ and $Y_{\mathbf{k},\sigma} = \text{sech}^2(\beta\xi_{\mathbf{k},\sigma} / 2)$. Notice that c_{ij} reduces to a scalar c in the s-wave case. The coefficient of the nonlinear term is $b = \sum_{\mathbf{k}} [X_{\mathbf{k},+} / (4\xi_{\mathbf{k},+}^3) - \beta Y_{\mathbf{k},+} / (8\xi_{\mathbf{k},+}^2)] |\Gamma_{\mathbf{k}}|^4$, while d has real and imaginary parts given by $d = \lim_{w \rightarrow 0} \sum_{\mathbf{k}} X_{\mathbf{k},+} [1 / (8\xi_{\mathbf{k},+}^2) + i\pi\delta(2\xi_{\mathbf{k},+} - w) / (2w)] |\Gamma_{\mathbf{k}}|^2$, where $\delta(x)$ is the Delta function. Notice that the damping term (imaginary part of d) vanishes for $\mu_+ \leq 0$, indicating an undamped dynamics for $\Lambda(x)$.

Since a uniform superfluid phase is more stable in the BEC side, we calculate analytically all coefficients in the BEC limit where $|\mu_{\pm}| \sim |\epsilon_b| / 2 \gg T_c$. We obtain $a = a_1 + a_2 = -Vm_+^2(2\mu_+ - \epsilon_b)a_F / (8\pi) + Vm_+ n_e a_F^2$, $b = b_1 + b_2 = Vm_+^3 a_F^3 / (16\pi) - Vm_+^2 (\partial n_e / \partial \mu_e) a_F^4$, $c = Vm_+^2 a_F / [8\pi(m_{\uparrow} + m_{\downarrow})]$, and $d = Vm_+^2 a_F / (8\pi)$. Here, e labels the excess type of fermions and n_e is the density of unpaired fermions. Through the rescaling $\Psi(x) = \sqrt{d}\Lambda(x)$, we obtain the equation of motion for a dilute mixture of weakly interacting bosons and fermions

$$\mu_B \Psi(x) + [U_{BB} |\Psi(x)|^2 + U_{BF} n_e(x)] \Psi(x) - \frac{\nabla^2 \Psi(x)}{2m_B} - i \frac{\partial \Psi(x)}{\partial t} = 0, \quad (7)$$

with bosonic chemical potential $\mu_B = -a_1/d = 2\mu_+ - \epsilon_b$, mass $m_B = d/c = m_{\uparrow} + m_{\downarrow}$, and repulsive boson-boson $U_{BB} = b_1 V / d^2 = 4\pi a_F / m_+$ and boson-fermion $U_{BF} = a_1 V / (dn_e) = 8\pi a_F / m_+$ interactions. This procedure also yields the spatial density of unpaired fermions given by $n_e(x) = [a_2/d + b_2 |\Psi(x)|^2 / d^2] / U_{BF} = n_e - 8\pi a_F (\partial n_e / \partial \mu_e) |\Psi(x)|^2 / m_+$. Since $\partial n_e / \partial \mu_e > 0$ the unpaired fermions avoid regions where the boson field $|\Psi(x)|$ is large. Thus, the bosons condense at the center and the unpaired fermions tend to be at the edges in a trap. Notice that, Eq. (7) reduces to the Gross-Pitaevskii equation for equal masses with $P = 0$ [31], and to the equation of motion for equal masses with $P \neq 0$ [21].

Furthermore, we obtain the boson-boson $a_{BB} = [1 + m_{\uparrow} / (2m_{\downarrow}) + m_{\downarrow} / (2m_{\uparrow})] a_F$ and boson-fermion $a_{BF} = 4m_B m_e / [m_+(m_B + m_e)] a_F$ scattering lengths, which reduce to $a_{BB} = 2a_F$ and $a_{BF} = 8a_F/3$ for equal masses [21, 31]. For a mixture of ${}^6\text{Li}$ and ${}^{40}\text{K}$, $a_{BB} \approx 4.41a_F$, and $a_{BF} \approx 2.03a_F$ when ${}^6\text{Li}$ is in excess, and $a_{BF} \approx 8.20a_F$ when ${}^{40}\text{K}$ is in excess. For a better estimate, higher order scattering processes are needed [32]. Since the effective boson-fermion system is weakly interacting, the BEC temperature is $T_c = \pi [n_B / \zeta(3/2)]^{2/3} / m_B$, where $\zeta(x)$ is the Zeta function and $n_B = (n - n_e) / 2$.

In summary, we analyzed the phase diagram of uniform superfluidity for two-species fermion mixtures (e.g. ${}^6\text{Li}$

and ${}^{40}\text{K}$) from the BCS to the BEC limit as a function of scattering parameter and population imbalance. We found that the zero temperature phase diagram of population imbalance versus scattering parameter is asymmetric for unequal masses, having a larger stability region for uniform superfluidity when the lighter fermions are in excess. This result is in sharp contrast with the symmetric phase diagram for equal masses. In addition, we found topological quantum phase transitions associated with the disappearance or appearance of momentum space regions of zero quasiparticle energies. Near the critical temperature, we derived the Ginzburg-Landau equation, and showed that it describes a dilute mixture of bosons (tightly bound fermions) and excess (unpaired) fermions in the BEC limit.

We thank NSF (DMR-0304380) for the support.

-
- [1] M. W. Zwierlein et al., *Science* **311**, 492 (2006).
 - [2] G. B. Partridge et al., *Science* **311**, 503 (2006).
 - [3] C. A. Regal et al., *Phys. Rev. Lett.* **92**, 040403 (2004).
 - [4] M. Bartenstein et al., *Phys. Rev. Lett.* **92**, 120401 (2004).
 - [5] J. Kinast et al., *Phys. Rev. Lett.* **92**, 150402 (2004).
 - [6] T. Bourdel et al., *Phys. Rev. Lett.* **93**, 050401 (2004).
 - [7] M. Köhl et al., *Phys. Rev. Lett.* **94**, 080403 (2005).
 - [8] G. B. Partridge et al., *Phys. Rev. Lett.* **95**, 020404 (2005).
 - [9] W. V. Liu and F. Wilczek, *Phys. Rev. Lett.* **90**, 047002 (2003).
 - [10] P. F. Bedaque et al., *Phys. Rev. Lett.* **91**, 247002 (2003).
 - [11] J. Carlson and S. Reddy, *Phys. Rev. Lett.* **95**, 060401 (2005).
 - [12] C. H. Pao et al., *Phys. Rev. B* **73**, 132506 (2006).
 - [13] D. T. Son and M. A. Stephanov, *Phys. Rev. A* **74** 013614 (2006).
 - [14] D. E. Sheehy and L. Radzihovsky, *Phys. Rev. Lett.* **96**, 060401 (2006).
 - [15] T. L. Ho and H. Zhai, *cond-mat/0602568*.
 - [16] A. Bulgac et al., *cond-mat/0602274*.
 - [17] Z.-C. Gu et al., *cond-mat/0603091*.
 - [18] H. Hu and X.-J. Lu, *cond-mat/0603332*.
 - [19] S. Sachdev and K. Yang, *cond-mat/0602032*.
 - [20] T. Mizushima et al., *Phys. Rev. Lett.* **94**, 060404 (2005).
 - [21] P. Pieri and G. C. Strinati, *Phys. Rev. Lett.* **96**, 150404 (2006).
 - [22] J. Kinnunen et al., *Phys. Rev. Lett.* **96**, 110403 (2006).
 - [23] W. Yi and L. M. Duan, *Phys. Rev. A* **73**, 031604 (2006).
 - [24] F. Chevy, *Phys. Rev. Lett.* **96**, 130401 (2006).
 - [25] T. N. De Silva and E. J. Mueller, *Phys. Rev. A* **73**, 051602(R) (2006).
 - [26] M. Haque and H. T. C. Stoof, *cond-mat/0601321*.
 - [27] V. N. Popov, *Functional Integrals and Collective Excitations*, Cambridge Univ. Press (1987)
 - [28] G. E. Volovik, *Exotic Properties of Superfluid ${}^3\text{He}$* , World Scientific, Singapore (1992).
 - [29] R. D. Duncan and C. A. R. Sá de Melo, *Phys. Rev B* **62**, 9675 (2000).
 - [30] J. R. Engelbrecht et al., *Phys. Rev. B* **55**, 15153 (1997).
 - [31] C. A. R. Sá de Melo et al., *Phys. Rev. Lett.* **71**, 3202 (1993).

- [32] D. S. Petrov et al., *J. Phys. B: At. Mol. Opt. Phys.* **38**, S645 (2005).